Co-Registration of Intra-Operative Photographs and Pre-Operative MR Images

Benjamin Berkels[1], Ivan Cabrilo[2], Sven Haller[2],
Martin Rumpf[1], Carlo Schaller[2]

[1]Institut für Numerische Simulation, Rheinische Friedrich-Wilhelms-Universität Bonn
[2]Hôpitaux Universitaires de Genève
`benjamin.berkels@ins.uni-bonn.de`

Abstract. Brain shift, i. e. the change in configuration of the brain after opening the dura mater, is a key problem in neuronavigation. We present an approach to co-register intra-operative microscope images with pre-operative MRI data to adapt and optimize intra-operative neuronavigation. The tools are a robust classification of sulci on MRI extracted cortical surfaces, guided user marking of most prominent sulci on a microscope image, and the actual variational registration method with a fidelity energy for 3D deformations of the cortical surface combined with a higher order, linear elastica type prior energy. Furthermore, the actual registration is validated on an artificial testbed and on real data of a neuro clinical patient.

1 Introduction

The development of medical imaging in the last decades quickly triggered intense interest from the medical world to translate this progress on the imaging side to clinical diagnostics and treatment planning. In that respect image registration and in particular recently also the fusion of 2D and 3D image data is a fundamental task in image–guided medical intervention. In [1] 2D photographs of human faces are registered with a triangulated facial surface extracted from MRI data using rigid deformations. A registration method for sparse but highly accurate 3-D line measurements with a surface extracted from volumetric planning data based on the consistent registration idea and higher order regularization is introduced in [2].

The matching of photographic images with pre-operative MRI data is a particular challenge in cranial neuronavigation. The photograph–MRI registration problem in the context of intracranial electroencephalography has been investigated via a control point matching approach in [3]. Recently, normalized mutual information has been applied for the rigid transformation co-registration of brain photographs and MRI extracted cortical surfaces [4]. A major limitation of note, however, is that due to the brain shift the surgeon's view of the operating site is not in a rigid transformation correspondence to pre-operative images. Indeed, standard intracranial neuronavigation devices do not correct for

this movement of brain [5]. The main contributions of this paper are a novel classification method for crease pattern such as sulci on implicit (cortical) surfaces and the actual 2D-3D registration method, where a non-rigid 3D deformation of the cortical surface is identified based on user marked sulci on photographs and the camera parameters.

2   Materials and Methods

The aim of this paper is to register a photograph of the exposed human cortex with the cortex geometry extracted from an MRI data set, see Fig. 1, using the sulci as fiducials. The main ingredients of the proposed approach are a sulci classification on the cortex geometry (Section 2.1) and on the photograph (Section 2.2), as well as a model that uses the two classifications to register photograph and cortical geometry (Section 2.3). The 2D digital photographs were taken intra-operatively after supratentorial craniotomy and durotomy, and before corticotomy, using a digital camera with 10 mega pixel resolution
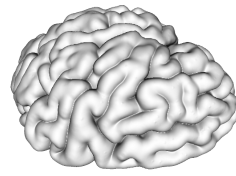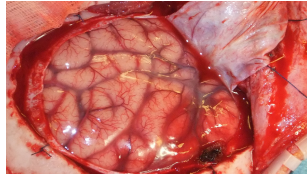

Fig. 1. Input photograph, MRI graph surface

positioned 20 cm above the craniotomy. The MR imaging was performed on a 3T MRI scanner. A T1-weighted MP2RAGE sequence ($1 \times 1 \times 1\ m^3$, $256 \times 256 \times 176$ matrix) was segmented into gray and white matter using BrainVoyager QX [6] and then converted into a signed distance function of the cortical surface using a fast marching method.

2.1   Sulci Classification on MRI Data

In this section, we describe how to classify creases on the contour surface of a 3D object $\mathcal{B} \subset \Omega$ represented via its signed distance function $d : \Omega \to \mathbb{R}$ on a computational domain Ω. In the application the object is a brain volume and the creases are the sulci on the cortical surface. We aim for a moment based analysis of the (cortical) surface $\mathcal{C} := \partial\mathcal{B}$ and define the zero moment shift of the
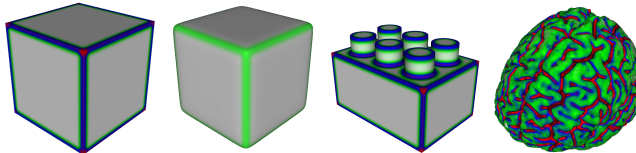

Fig. 2. Moment-based classification

implicit surface $\mathcal{C}$ as follows $M_\epsilon^0[\mathcal{B}](x) = \frac{1}{|B_\epsilon(x)|} \int_{B_\epsilon(x)} d(y)(y - x)\mathrm{d}y$ which returns larger values in flat regions of $\mathcal{C}$ than in edge regions and even smaller near corners (cf. [7] for a related moment based classification on explicit surfaces). We define the scalar classification $\mathbf{C}(x) = g_\beta\left(\|M_\epsilon^0[\mathcal{B}](x)\|/\epsilon^2\right)$, where $g_\beta(t) = \frac{1}{1+\beta t^2}$. Fig. 2 illustrates the behavior of the classifier $\mathbf{C}$ on three simple shapes and a

cortical surface extracted from an MRI using a white-green-blue-red color coding. We observe a robust distinction for a single set of parameters ($\beta = 20$ and $\epsilon = 8h$ or $4h$, where h denotes the grid width).

2.2   Generation of Annotated Cortex Photographs

Essential problems for the classification of sulci on photographs are additional structures and their misinterpretation. Most prominent are cortical veins, which in addition partially occlude sulci (these veins are almost invisible in MRI in the used MP2RAGE sequence). On this background we here confine to a still manual marking of sulci by an expert who is supported by the results of a prior automatic pre-classification of sulci based on learned discriminative dictionaries, cf. Fig. 3, where the method from [8] is used.
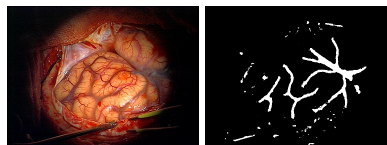

Fig. 3. Cortex photograph and dictionary based pre-classification

2.3   Registration of Photograph and Cortex Geometry

The co-registration of an MRI extracted cortical surface $\mathcal{C} \subset \mathbb{R}^3$ and a photograph to compensate for effects such as the brain shift is based on a co-registration of the sulci classifiers on $\mathcal{C}$ and the photograph. To this end, we suppose $\mathcal{C}$ to be described as a graph

$$\mathcal{C} = \{(x, z(x)) \in \mathbb{R}^3 | x \in \omega\}$$

with parameter domain $\omega \subset \mathbb{R}^2$ and graph function $z : \omega \to \mathbb{R}$. We are interested in a local registration described by the craniotomy, where such a graph representation can be easily derived from the signed distance function used in Section 2.1. Furthermore, let $g \in L^2(\Omega)$ denote the sulci classifier on the photograph domain Ω (cf.
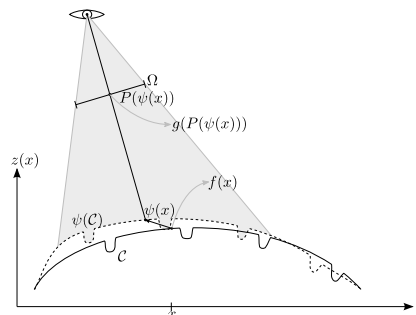

Fig. 4. Geometric configuration

Section 2.2), and $f \in L^2(\omega)$ the corresponding classifier on the cortical surface given as a function on the parameter domain ω, obtained by a suitable clamping of **C** and rescaling of the values to the unit interval $[0, 1]$ (cf. Section 2.1). Both classifiers are supposed to be close to 1 in the central region of the sulci and small outside. Finally, we denote by $P : \mathbb{R}^3 \to \Omega$ the projection of points in $\mathbb{R}^3$ onto the image plane Ω derived from known camera parameters. Let us remark that we thereby implicitly rule out self occlusions of the graph surface $\mathcal{C}$ under the image plane projections. Now, we ask for a deformation $\Psi : \omega \to \mathbb{R}^3$ defined on the parameter domain ω of the graph function z that matches $\mathcal{C}$ to its deformed configuration represented under the projection P in the photograph. Thereby, matching is encoded via the coincidence of the surface classifier $f(x)$ on the MRI

described cortical surface and the image classifier $g(P(\psi(x)))$ evaluated at the projected deformed position $P(\psi(x))$ for all x on the parameter domain ω. Thus, proper matching can be encoded via the minimization of the matching energy

$$E_{\mathrm{match}}[\psi] = \frac{1}{2} \int_\omega [g(P(\psi(x))) - f(x)]^2 A(x)\mathrm{d}x$$

based on a surface integral over $\mathcal{C}$ with the area element $A(x) = (1+|\nabla z(x)|^2)^{\frac{1}{2}}$, to consistently reflect the cortex geometry. In the overall variational approach the matching energy is complemented by a suitable elastic regularization energy, which acts as a prior on admissible deformations ψ. Here, we consider the second order, elastic energy

$$E_{\mathrm{reg}}[\psi] = \frac{1}{2} \int_\omega |\Delta\psi_1(x)|^2 + |\Delta\psi_2(x)|^2 + |\Delta\psi_3(x) - \Delta z(x))|^2 \mathrm{d}x.$$

Note that a simple first order regularization like the Dirichlet energy of the displacement $\psi - (\cdot, z(\cdot))$ is not sufficient since matching information is mostly given on a low dimensional subset where proper nonlinear extrapolation is required and bending modes play an important role. Obviously, E_{reg} is rigid body motion invariant (cf. [9]). Finally, we combine the matching energy E_{match} and the regularization energy E_{reg} to the total energy functional $E[\psi] = E_{\mathrm{match}}[\psi] + \lambda E_{\mathrm{reg}}[\psi]$ on deformations ψ encoding the deformation of the cortical surface $\mathcal{C}$, where λ is a positive constant controlling the strength of the regularization.

To minimize the objective functional we use a time discrete regularized gradient descent taking into account a suitable step size control combined with a cascadic descent approach to handle the registration in a coarse to fine manner. The first variation necessary for the descent algorithm is

$$\langle E'[\psi], \zeta \rangle = \int_\omega [g(P(\psi(x))) - f(x)]\nabla g(P(\psi(x))) \cdot DP(\psi(x))\zeta(x)A(x)\mathrm{d}x$$
$$+ \lambda \int_\omega (\Delta^2\psi_1, \Delta^2\psi_2, \Delta^2(\psi_3 - z)) \cdot \zeta\mathrm{d}x,$$

where the natural boundary conditions $\partial_\nu \Delta\psi = \Delta\psi = 0$ on $\partial\omega$ for the normal ν on $\partial\omega$ are considered and ψ is initialized as the identity on $\mathcal{C}$, i. e. $\psi(x) = (x, z(x))$. For the spatial discretization we consider bilinear Finite Elements on a rectangular mesh overlaying ω and Ω, and approximate the bi-Laplacian Δ^2 by the squared standard discrete Laplacian $\Delta_h^2 = M^{-1}LM^{-1}L$. Here, M and L denote the standard (lumped) mass and stiffness matrices, respectively.

3   Results

We have applied our registration approach both to test data and to real data. For the test data a cortical surface segmented on a 3D MRI data set has been taken as input together with an image generated from this surface via a given
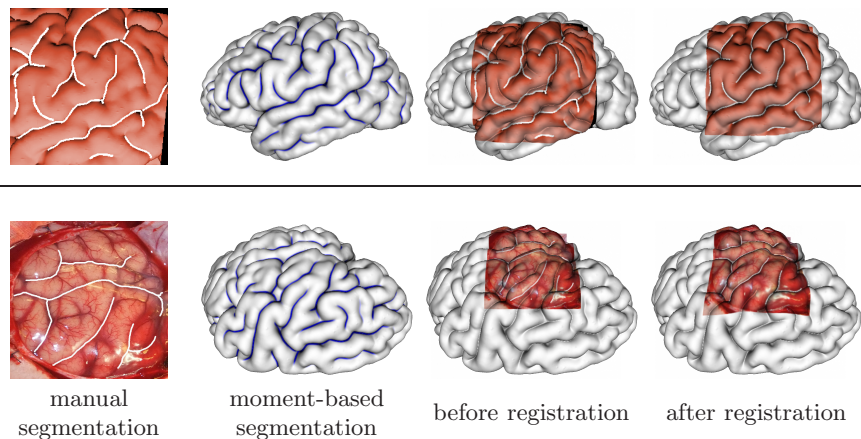
| manual
segmentation | moment-based
segmentation | before registration | after registration |

Fig. 5. Both for the test data (top row) and the pair of a true photograph and an MRI extracted cortical surface (bottom row) we show (from left to right) the input image with marked sulci (computed image and real photograph respectively), the sulci classification on the 3D cortical surface segmented from MRI data, the initial misfit of the sulci marking on the 2D image projected on the cortical surface overlaying the cortical surface itself, and the final registration result.

projection concatenated with an additional 3D nonrigid deformation. Then on the projected image selected sulci have been marked by hand. This pair of input data together with the computed registration result are depicted in Fig. 5.

Furthermore, we considered a photograph of the brain surface seen through a left fronto-temporo-parietal craniotomy performed in a patient before placement of a subdural electrode grid for investigation of drug-resistant cryptogenic epilepsy. We segmented sulci using the procedure in Section 2.2. This is then registered via the proposed approach with the cortical surface extracted from the corresponding pre–interventional 3D MRI data. Again input data and achieved registration are shown in Fig. 5.

4   Discussion

We have proposed a novel method for the registration of photographs (2D) of the brain with the cortical surface extracted from 3D MRI data. The method turns out to be effective and robust both on test and on real data. It can be considered as an alternative to intra-operative MRI allowing subsequent co-registration with neuronavigation [10]. Currently, we aim for a validation study with an increased number of cases considering also data of patients with substantially smaller craniotomies.

Furthermore, there is potential, that the iterative 2D/3D surface registration of digital images together with morphological 3D MRI data sets will enable to build up a "dictionary" of brain surface features. Ultimately, the creation of such a dictionary might, to a certain extent, permit "intelligent" automatic recognition

of brain surface features, where the 2D brain surface, seen through the intra-operative microscope standardly used during intra-cerebral procedures, would directly be co-registered to pre–interventional 3D MRI data.

As already discussed, the sensitivity of MRI and photography is substantially different for different anatomic structures, e. g. veins are very prominent on images yet not on the MRI modality used here. One could incorporate multiple MRI sequences and fuse vein sensitive images with the present images to improve the registration results. Finally, let us remark that one could also consider stereo photographs of the deformed surface to improve the methods performance. In that respect our approach can easily be adapted summing over copies of the matching energy.

References

1. Clarkson MJ, Rueckert D, Hill DLG, Hawkes DJ. Using Photo-Consistency to Register 2D Optical Images of the Human Face to a 3D Surface Model. IEEE Trans Pattern Anal Mach Intell. 2001;23(11):1266–1280.
2. Bauer S, Berkels B, Ettl S, Arold O, Hornegger J, Rumpf M. Marker-less Reconstruction of Dense 4-D Surface Motion Fields using Active Laser Triangulation from Sparse Measurements for Respiratory Motion Management. In: Medical Image Computing and Computer-Assisted Intervention (MICCAI 2012). vol. 7510 of Lect Notes Computer Sci; 2012. p. 414–421.
3. Dalal SS, Edwards E, Kirsch HE, Barbaro NM, Knight RT, Nagarajan SS. Localization of neurosurgically implanted electrodes via photograph–MRI–radiograph coregistration. J Neurosci Methods. 2008;174(1):106–115.
4. Wang A, Mirsattari SM, Parrent AG, Peters TM. Fusion and visualization of intraoperative cortical images with preoperative models for epilepsy surgical planning and guidance. Comput Aided Surg. 2011;16(4):149–160.
5. Reinges MHT, Nguyen HH, Krings T, Hütter BO, Rohde V, Gilsbach JM. Course of brain shift during microsurgical resection of supratentorial cerebral lesions: limits of conventional neuronavigation. Acta Neurochir (Wien). 2004;146(4):369–377.
6. Fischla B, Serenob MI, Dalea AM. Cortical Surface-Based Analysis: II: Inflation, Flattening, and a Surface-Based Coordinate System. Neuroimage. 1999;9(2):195–207.
7. Clarenz U, Rumpf M, Telea A. Robust Feature Detection and Local Classification for Surfaces based on Moment Analysis. IEEE Trans Vis Comput Graph. 2004;10(5):516–524.
8. Berkels B, Kotowski M, Rumpf M, Schaller C. Sulci Detection in Photos of the Human Cortex Based on Learned Discriminative Dictionaries. In: Scale Space and Variational Methods in Computer Vision. Lect Notes Computer Sci; 2011. .
9. Modersitzki J. Numerical Methods for Image Registration. Oxford University Press; 2004.
10. Kuhnt D, Bauer MH, Nimsky C. Brain shift compensation and neurosurgical image fusion using intraoperative MRI: current status and future challenges. Crit Rev Biomed Eng. 2012;40:175–85.